



UNIVERSITY OF LEEDS

This is a repository copy of *Relationship between bowl-shaped clastic injectites and parent sand depletion; implications for their scale invariant morphology and composition*.

White Rose Research Online URL for this paper:  
<http://eprints.whiterose.ac.uk/147966/>

Version: Accepted Version

---

**Article:**

Cobain, SL, Hodgson, DM [orcid.org/0000-0003-3711-635X](https://orcid.org/0000-0003-3711-635X), Peakall, J [orcid.org/0000-0003-3382-4578](https://orcid.org/0000-0003-3382-4578) et al. (1 more author) (2019) Relationship between bowl-shaped clastic injectites and parent sand depletion; implications for their scale invariant morphology and composition. Geological Society Special Publications, 493. ISSN 0305-8719

<https://doi.org/10.1144/SP493-2018-80>

---

© 2019 The Author(s). This is an author produced version of an article published in Geological Society Special Publications. Uploaded in accordance with the publisher's self-archiving policy.

**Reuse**

Items deposited in White Rose Research Online are protected by copyright, with all rights reserved unless indicated otherwise. They may be downloaded and/or printed for private study, or other acts as permitted by national copyright laws. The publisher or other rights holders may allow further reproduction and re-use of the full text version. This is indicated by the licence information on the White Rose Research Online record for the item.

**Takedown**

If you consider content in White Rose Research Online to be in breach of UK law, please notify us by emailing [eprints@whiterose.ac.uk](mailto:eprints@whiterose.ac.uk) including the URL of the record and the reason for the withdrawal request.



[eprints@whiterose.ac.uk](mailto:eprints@whiterose.ac.uk)  
<https://eprints.whiterose.ac.uk/>

1 **Relationship between bowl-shaped clastic injectites and parent sand**  
2 **depletion; implications for their scale invariant morphology and**  
3 **composition**

---

4 **Abbreviated title: Bowl-shaped injectites and depleted parent sand**

5 S.L. Cobain, <sup>1\*</sup>, D.M. Hodgson<sup>1</sup>, J. Peakall<sup>1</sup>, S.Y. Silcock<sup>2</sup>

6 <sup>1</sup>School of Earth and Environment, University of Leeds, Leeds, LS2 9JT, UK

7 <sup>2</sup>Equinor Production (UK) Limited, Equinor House, Prime Four Crescent, Kingswells, Aberdeen,  
8 AB15 8QG, United Kingdom

9 \*Present address: BP, ICBT Sunbury, Chertsey Road, Sunbury on Thames, TW16 7LN, UK  
10 (Sarah.Cobain@bp.com)

11

12 **Abstract**

13 3D seismic reflection data provides a means to assess the impact of injection on parent sands,  
14 and to quantify the character of the resulting injectite networks. The morphology of a series  
15 of large injectite structures hosted in the Palaeocene Lower Lista Formation were mapped  
16 using broadband 3D seismic data from the North Sea to investigate their relationship with  
17 parent sands. Fourteen bowl-shaped structures were identified within the Lista Formation in  
18 the study area (60-85 m in height, and 200-900 m in width). Sand is absent (below resolution)  
19 below these large-scale bowls, suggesting that the parent sand is the underlying Maureen  
20 Formation and sand 'welds' formed, rather than sand-prone channelised deposits within the  
21 Lista Formation.

22 Identification of injectite networks can be ambiguous, which impacts geological model  
23 development. Observations from exhumed systems and core, offers high resolution insights  
24 into the complexity of injectite networks. To advance our understanding of this scale gap, we

25 argue for injectites being scale invariant in their shape and grain-size. This permits the  
26 application of outcrop-scale knowledge to seismic-scale interpretation. The demonstrable  
27 depletion of parent sands, and their scale invariance, can be applied to basin-fills worldwide  
28 to reduce uncertainties of the impact of sand injectites on hydrocarbon reservoirs.

29

30 Keywords: clastic injectites, dykes, sills, North Sea, scale invariance

31

32 Clastic injectites are the products of the forceful intrusion of sediment-rich flows into a host  
33 lithology (Jolly and Lonergan, 2002). The source of the intrusive material therefore, must  
34 undergo some form of sand depletion (Løseth *et al.*, 2012). In core, outcrop, or seismic  
35 datasets it is challenging to associate injectite networks with their parent sand unit (e.g.  
36 Cobain *et al.* 2018) unless the connection is observed directly, and even more difficult if the  
37 parent body is partially depleted of sand. In the subsurface, identification of injectites and  
38 their parent sand is important for modelling fluid flow pathways between bodies of sand, and  
39 prediction of the reservoir quality of the injectites.

40 Here, we present a case study of clastic injectites and an associated potential area of sand  
41 depletion of the underlying stratigraphic unit, from the North Sea. Using a high resolution  
42 broadband 3D seismic dataset offers the opportunity to map injectite bodies, identify the  
43 likely parent sands, and to quantify their morphology and dimensions. The ability to map and  
44 quantify the large-scale injectites in 3D seismic data is an advantage over exhumed injectites,  
45 at outcrop (2D) and in core (1D). However, these data illustrate that there is both a far greater  
46 complexity in injectites than is often accounted for, and that they occur over several orders  
47 of magnitude. From this, we argue that in terms of geometry, injectites might be scale  
48 invariant in form and grain-size. Therefore, injectite geometry can be compared between  
49 systems. If there is scale invariance of injectite geometry this could improve reservoir  
50 modelling and the appropriate use of outcrop analogues.

51 Our aim is to map a series of injectites within the study area and consider their origin and sub-  
52 seismic characteristics. To meet this aim, the following objectives were addressed: i)  
53 documentation of the dimensions and shapes of injectites within the study area, ii) discussion  
54 of the timing and parent sand for the injectites, iii) consideration of whether injectites can be  
55 scale invariant by scale and composition, and iv) discussion of the implications of scale  
56 invariance on the use of outcrop analogues for injectites identified in the subsurface.

57

## 58 **Geological setting**

59 The North Sea case study area is composed of Palaeocene sediments that onlap Devonian  
60 basement and Late Cretaceous/Early Palaeocene chalk landward (Fig. 1) (Ahmadi *et al.*, 2003).  
61 The lowermost Palaeocene sands are interpreted to be a series of massive, stacked,  
62 submarine channel and fan deposits (Maureen Formation; Mudge and Copestake, 1992;  
63 Mudge, 2014). Sands were fed via deltas and through slope channel systems from the north-  
64 west (Galloway *et al.*, 1993) to a submarine fan. A thick (>600 m) hemipelagic mudstone  
65 succession (Lista Formation; Ahmadi *et al.*, 2003) directly overlies the submarine fan and  
66 channel-fill sands, which formed during a period of relative sea-level rise. Located within these  
67 mudstones are a series of sand-prone channelised systems (Ahmadi *et al.*, 2003). Injected and  
68 remobilised sands have been interpreted in the Lista Formation mudstone in many locations  
69 in the North Sea (e.g. Cheret and Carrillat, 2004; de Boer *et al.*, 2007; Satur and Hurst, 2007;  
70 Kilhams *et al.*, 2012). This study focuses on the architecture and source of clastic injectites in  
71 the Lower Lista Formation that directly overlies the Maureen Formation (Fig. 1B).

## 72 **Methodology**

### 73 **Seismic mapping**

74 The study covers a 5.75 km long, and 2.12 km wide (~12 km<sup>2</sup>) sub-area of a high resolution 3D  
75 broadband seismic dataset, focussing on the Lower Lista Formation (Figs. 2A and 2B). The  
76 advantage of using broadband seismic data (or multi-sensor towed streamer technology) is  
77 the improved imaging of complex geometries, where it is possible to image Lista sandstone  
78 with higher frequencies and less sidelobes within the data, resulting in a more accurate  
79 interpretation (Østmo *et al.*, 2014). The 3D broadband seismic survey has been time migrated  
80 with a standard anisotropic 3D Kirchhoff migration, was interpreted with in-line (IL),  
81 northwest-southeast orientation, and cross-line (XL), northeast-southwest orientation, and

82 has a line spacing of 6.25 metres by 6.25 metres. A positive peak event (blue-black reflection)  
83 represents a downward increase in acoustic impedance whereas a negative trough (orange-  
84 red reflection) represents a downward decrease in acoustic impedance (Figs. 2C – 2F).  
85 In the study area, reflections are more brightly imaged on the near angle stack (5°-17.5°), and  
86 were chosen for mapping. Mapped sands are penetrated directly by two vertical wells  
87 allowing them to be calibrated with the well logs (Fig. 3). Initially, the base of the sand bodies  
88 were mapped on every 16<sup>th</sup> IL and XL (100 m) and then from the grid created by this method  
89 every IL and XL was mapped where correlating between lines was problematic. Arbitrary lines  
90 were used where correlating between adjacent lines was ambiguous. Mapped sands crosscut  
91 stratigraphy, display both low and high angles of dip (defined as <20° and >20° respectively  
92 (Hurst *et al.*, 2011)), and form bowl-shaped structures in 3D (Fig. 2). A major uncertainty with  
93 mapping injectites is that steeply dipping injectites (usually >60° (Jackson *et al.*, 2011)) are not  
94 imaged on seismic data. However, because the dataset used in this study is of such high  
95 resolution, it is possible to infer whether an absence or break of seismic reflection is due to  
96 steeply dipping sand units. The complicated nature of injectite geometries, which locally  
97 includes the separation of a single mappable sand body into several thinner sand units on  
98 different stratigraphic levels, can produce a chaotic seismic response. Where this occurred  
99 either the brightest reflector was selected, or when no obviously bright reflector was present  
100 the lowermost reflector was selected (e.g. Fig. 2F).

101

## 102 **Results and analysis**

### 103 **Seismic mapping**

104 Fourteen bowl structures were mapped in detail over the ~12 km<sup>2</sup> study area, including bright  
105 reflections interpreted to be sands that connect to, or sit in-between, bowl-shaped structures.  
106 These structures are shown to crosscut stratigraphy at high angles (Fig. 2C-F) and internally

107 have chaotic seismic response. After being mapped in 3D, 2D seismic profiles were taken at  
108 intervals of 50 m along both ILs and XLs for quantitative analysis (Table 1); some results are  
109 displayed as crossplots (Fig. 4). The key geometric parameters measured for each individual  
110 bowl include: i) plan view area as an aerial parameter ( $m^2$ ), defined where the steeply dipping  
111 sandstone bodies pass abruptly into sills concordant with host strata; ii) height of bowl,  
112 defined as the vertical extent (m) from the base (lowest depth) to the abrupt change between  
113 steeply dipping side and shallowly dipping sill; and iii) the width of each bowl through both IL  
114 and XL sections, defined as the horizontal extent (m) along both IL and XL inside the aerial  
115 extent of the bowl (Table 1). Measurements provided have an uncertainty of  $\pm 6.25$  m  
116 horizontally (bin spacing) and vertically of  $\pm 12$  m (vertical resolution). Internal sand  
117 geometries and sand thicknesses are difficult to estimate because well calibrations show  
118 these are likely clustered zones of thin sands (Loneragan *et al.*, 2007) as opposed to a single,  
119 thick, high net-to-gross body (Huuse *et al.*, 2004; de Boer *et al.*, 2007). Most of the bowl  
120 structures are between 60 and 85 metres in height. Maximum measured widths are between  
121 200 and 900 metres (Fig. 2), with an average width of 574 metres. The vertical distance  
122 between the top of the Maureen Formation sandstone and the base of the lowermost section  
123 of each bowl ranges from zero (bowl 8a in contact with Maureen Formation; Figure 2D) to 89  
124 metres (bowl 9). There are 2 distinct stratigraphic horizons above the Maureen Formation  
125 along which sands abruptly change from steeply dipping and discordant to concordant with  
126 stratigraphy (Figs. 2C and 2D). Quantitative data show that the degree of variability between  
127 the bowls is low to moderate. There is a strong correlation between the width and height of  
128 bowl structures (Fig. 4B). These sands are interpreted as clastic injectites due to their  
129 geometry (bowl-shaped and cross-cutting stratigraphy at high angles) and apparent  
130 relationship with underlying sand unit. Sands at high angles to stratigraphy have recently been  
131 described by Totake *et al.*, (2018) where sand slices were mapped along thrust fault planes;  
132 in cross-section there is some resemblance to sands in this study at high angles to surrounding

133 strata. This, however, is discounted as a possibility as mapped sands herein form bowl  
134 structures in 3D, and stratigraphy either side of the sands is not displaced.

135

## 136 **Discussion**

### 137 **Source of North Sea case study injectites**

138 The parent sand of these injectites is a source of debate; the two possibilities are either the  
139 Lista Sandstones, a series of sand-prone channelised deposits within the Lista Formation (Fig.  
140 1), or the underlying Maureen Formation, which comprises stacked lobe and channel deposits  
141 (Fig. 1). Provenance studies would confirm the parent sand from which injectites are sourced,  
142 however, here we argue for injectite-parent relationship. The mapped bowl structures  
143 presented here show a strong spatial affinity with the underlying Maureen Formation sands,  
144 with some bowls showing direct contacts at their base with the Maureen Formation sands  
145 (e.g. Bowl 8a; Fig. 2D). Additionally, the location of the mapped bowls overlie areas where  
146 there is a seismic pinchout or absence of the underlying Maureen Formation (Figs. 2A, 2C, 2D  
147 and 5). In cross section, the absence of Maureen Formation sands resembles channel incision  
148 (Fig. 5). One explanation for this pinchout is the presence of a mud-filled channel system.  
149 However, removal by a channel would mean a markedly different orientation (WSW-ENE and  
150 curving northwards) to all other channels along the same palaeoslope, which have a  
151 palaeoflow of west-to-east (Mudge, 2014). Furthermore, in plan view, the mapped pinchouts  
152 are not in a channel form. For example, Figure 2A shows the Maureen Formation pinchout  
153 narrowing in planform, whereas a channel would be expected to have a more consistent  
154 along-axis width. An alternative explanation is that the lack of Maureen Formation sands in  
155 this area is the result of depletion through the remobilisation and injection of sand into the  
156 overlying Lista Formation. The spatial relationship between the absence of Maureen  
157 Formation and the presence of overlying large bowl structures, the abrupt pinchout of the



158 Maureen Formation, and the connection with the overlying injectites, support this  
159 interpretation. The apparent absence of Maureen Fm. sand beneath the injectite bowls points  
160 to significant withdrawal from the parent sands, and the possibility that 'sand welds' formed.  
161 In diapiric systems, a salt or mud weld is a surface (or thin zone) that marks the complete, or  
162 near complete, movement of salt or mud (Jackson and Cramez, 1989). In a similar way, the  
163 complete withdrawal of sand and redistribution into an injectite network could result in a  
164 sand weld forming; and a welded surface that could separate concordant, but unconformable,  
165 strata. Once a sand weld forms beneath an injectite, it will cease to be supplied with new  
166 material, and injectite propagation will cease. In the case of the Maureen Fm., the resolution  
167 of the data does not permit us to confidently define whether a complete (remnant sand 0 m  
168 thick) or incomplete (remnant sand 0-50 m) weld developed (*sensu* Hudec and Jackson, 2011).  
169 However, the mapping of the Maureen Fm. (Fig. 2) does reveal development of a  
170 discontinuous sand weld (*sensu* Hudec and Jackson, 2011).

171

## 172 **Origin of overpressure**

173 Overpressure is a key factor required to generate clastic injectites (Jolly and Lonergan, 2002).  
174 For this North Sea case study, the overpressure is suggested to be generated from: i)  
175 depositional sands being encased in low permeability mudstones, and ii) influx of  
176 hydrocarbons into sandstone units (Ahmadi *et al.*, 2003). Fluid pressures within the relatively  
177 shallow sandstones at the time of oil migration would have been near hydrostatic (Chiarelli  
178 and Richy, 1984; Barnard and Bastow, 1991; Kubala *et al.*, 2003). Fluid migration may not only  
179 have provided the source for overpressure, but potentially could have been the trigger  
180 mechanism needed for the initiation of clastic intrusion (e.g. Vigorito and Hurst, 2010;  
181 Monnier *et al.*, 2014; Cobain *et al.*, 2015, 2017). Other trigger mechanisms, such as seismicity,  
182 are also viable (e.g., see Cobain *et al.*, 2017).

### 183 **Timing of injectites**

184 Hydrocarbon migration from the Beryl Embayment into the up-dip Palaeocene sands is  
185 constrained to between 55 and 65 Ma and is known to be post calcite cementation (Ahmadi  
186 *et al.*, 2003). Constraints on the timing of the process of injection are limited, however the  
187 maximum vertical height of a single intrusion structure is 152 m, indicating a minimum burial  
188 depth of at least this amount prior to intrusion. Although the sands within the Lower Lista  
189 Formation are relatively shallow compared to some injectite complexes, they have undergone  
190 some burial and compaction since remobilisation and deposition. The constraints on the  
191 timing of this process are limited and the values presented herein have not been  
192 decompacted. The measured vertical heights in features, therefore, represent a minimum  
193 burial depth (Huuse *et al.*, 2004; Parize *et al.*, 2007).

194

### 195 **Scale invariance in injectite and the suitability of analogues**

196 Sand(stone) injectites have been reported on scales ranging from millimetres in length and  
197 thickness (Goodall *et al.*, 1999; Duranti *et al.*, 2002; Hurst *et al.*, 2011) to 10s metres thick and  
198 laterally extensive for kilometres (Huuse *et al.*, 2004; Hurst *et al.*, 2005, 2011; Hubbard *et al.*,  
199 2007; Cartwright, 2010; Cobain *et al.*, 2017). For example, km-scale bowl-shaped injectites  
200 have been identified and described in a number of oilfields, including the Volund (Townesley  
201 *et al.*, 2012; Schwab *et al.* 2015) and the Gamma Fields (Huuse *et al.*, 2007). They can share  
202 morphological similarities in 2D, and commonly have a narrow grain-size range (Fig. 7)  
203 attributed to preferential fluidisation of very fine sand over other grainsize types (Cobain *et*  
204 *al.*, 2015). The common occurrence of bowl shapes and fine grain size identified in injectites,  
205 along with scales ranging by orders of magnitude, suggests that injectites are scale invariant  
206 in their shape and composition; in other words injectite morphology and grain-size do not  
207 change when length scales are multiplied by a common factor. This characteristic could be  
208 critical in helping to predict and model sub-seismic scale injectite sands, and to identify

209 appropriate analogues from higher resolution data that can offer the chance to better  
210 understand process and product relationships in injectite networks. However, why should  
211 injectites be scale invariant in their shape?

212 The scale invariance of sand(stone) injections in sedimentary basins is attributed to the host  
213 lithology being one of the main factors determining the geometry and architecture of an  
214 intrusion as it propagates (see Figure 2 of Cobain *et al.*, 2015). In a similar way, faults and  
215 fractures are considered to be scale invariant (e.g. Scholz and Aviles, 1986; Schulz *et al.*, 2010)  
216 as a function of the host lithology (e.g. Wibberley *et al.*, 1999; Schultz *et al.*, 2010).  
217 Furthermore, work has shown that the style of sand intrusions into fault zones varies as a  
218 function of lithology (Palladino *et al.*, 2018). Previous research on intrusion dynamics has  
219 focussed primarily on igneous systems (McCaffrey and Petford, 1997; Thomson, 2007;  
220 Thomson and Schofield, 2008; Schofield *et al.*, 2012a; Magee *et al.*, 2015). However, similar  
221 geometries observed in both igneous and sedimentary intrusions suggest that emplacement  
222 mechanisms are comparable and controlled by the same external parameters (Cartwright *et*  
223 *al.*, 2008; Polteau *et al.*, 2008; Mourgues *et al.*, 2012). It should be noted however, that  
224 although mechanisms of emplacement may be comparable, rates of emplacement are likely  
225 quite different between clastic injections and igneous intrusions (e.g., Ross *et al.*, 2014;  
226 Sigmundsson *et al.*, 2015). Properties of host lithology that affect intrusion morphology during  
227 emplacement include the propensity for brittle behaviour *versus* non-brittle (Schofield *et al.*,  
228 2012a), the homogeneity of the host strata (Jolly and Lonergan, 2002), and the principal stress  
229 orientation (Jolly and Lonergan, 2002; Rowe *et al.*, 2002). As it is primarily the host lithology  
230 that controls final intrusion architecture, research and literature for scale invariance within  
231 igneous intrusions are utilised here.

232 Scale invariance over several orders of magnitude is recognised in igneous intrusions. One  
233 example is 'broken bridges', a distinctive morphology within igneous intrusions that has been  
234 well documented from centimetres up to several metres at outcrops (Nicholson and Pollard,

235 1985; Bussel, 1989). Schofield *et al.* (2012b) recognised that broken bridges developed  
236 between elongate magma lobes in the Faroe-Shetland Basin on a seismic scale of at least 10's  
237 of metres in height and with lateral extents of over several kilometres. Field data have also  
238 been used to test dimensional scaling and mechanical models, where a range of power-law  
239 scaling relationships for different types of intrusive structures can predict geometry for  
240 laccoliths and thickness-to-length relationships for mafic sills (Cruden and Bungler, 2010)  
241 implying scale invariance.

242 Experimental modelling also assumes scale invariance, where the use of dimensionless  
243 numbers demonstrates geometric and kinematic similarities between model and its natural  
244 prototype. This was first recognised by Hubbert (1937), and since then the principles of  
245 dimensional analysis of scaling have been used in many experiments replicating natural  
246 geological processes (Hubbert, 1951; Hubbert and Willis, 1957; Mourgues and Cobbold, 2003;  
247 Kavanagh *et al.*, 2006; Rodrigues *et al.*, 2009; Gressier *et al.*, 2010). For clastic injectites  
248 specifically, Rodrigues *et al.* (2009) and Mourgues *et al.* (2012) both successfully recreated  
249 injectite geometries comparable to those in nature that can be up to several kilometres in size  
250 (Vigorito and Hurst, 2010), yet experimentally may only be several centimetres. These  
251 experiments support injectite morphologies being scale invariant where outside factors, such  
252 as host rock lithology, fluid pressure, and principle stress orientation, are at a scaled  
253 equivalent both geometrically and kinematically (Rodrigues *et al.*, 2009; Mourgues *et al.*,  
254 2012).

255 The scale invariance of clastic injectites permits outcrop-scale data to be upscaled and applied  
256 to support seismic-scale interpretations. Therefore, the injectites at outcrop could be seismic  
257 forward modelled to aid recognition of injectites in reflection seismic data. Previously, the use  
258 of outcrop studies of injectites as analogues for subsurface examples has been limited to cases  
259 where the outcrop itself is of seismic scale (Surlyk and Noe-Nygaard, 2001; Vigorito *et al.*,

260 2008; Scott *et al.*, 2009, 2013; Vigorito and Hurst, 2010); an approach that limits the range of  
261 usable analogues and may ultimately mean inappropriate geometries used as analogues.

262

### 263 **Implications for hydrocarbon exploration**

264 Subsurface remobilisation and injection of sand has significant consequences on reservoir  
265 architecture, geometry, and porosity and permeability, which impact hydrocarbon recovery.

266 In this North Sea case study, the procedure has been employed to provide unequivocal  
267 evidence for the origin of the sand bodies mapped in the Lower Lista Formation shale to be  
268 clastic injectites and not of primary deposition. Moreover, there is likely more complexity to  
269 those sand bodies than can be observed in the reflection seismic data. Therefore, a larger  
270 volume of sub-seismic injectites, and hence greater volume of sand and connectivity, is likely  
271 present than would be predicted from seismic data alone (Fig. 8).

272 As more exploration drilling in the North Sea is specifically targeting clastic injectite complexes  
273 (de Boer *et al.*, 2007; Schwab *et al.*, 2015), having the ability to map and interpret injected  
274 sandstones and predict their sub-seismic distribution accurately is crucial to achieve economic  
275 viability of drilling and production from such fields. Increasing our understanding of the  
276 architecture of clastic injectites will allow more accurate interpretation during exploration,  
277 and more informed placement of production wells, increasing the economic viability of  
278 reservoirs (Fig. 8).

### 279 **Conclusions**

280 The broadband seismic survey data from this North Sea case study, combined with nearby  
281 well logs, were used to map in detail the 3D geometries of clastic injectites over a sub-area of  
282 ~12 km<sup>2</sup>. Fourteen bowl structures were identified, some of which showed a direct connection  
283 with the underlying Maureen Formation. Where this direct connection occurs, the Maureen  
284 Formation is partly absent, suggesting sand depletion as clastic material is forcibly injected

285 upwards into the Lower Lista Formation forming the sand bodies mapped and interpreted as  
286 injectites, and that sand welds developed. This is a rare case where, in the subsurface, the  
287 parent unit can be confidently associated with clastic injectites. The impact of injectites on  
288 hydrocarbon reservoirs, as well as an increase in the industry targeting unconventional or  
289 complex reservoirs, means that the need for this knowledge and understanding has never  
290 been so pertinent.

291 The bowl-shaped morphology of the large seismically resolvable structures, and the common  
292 grain-size of similar geometries across several orders of magnitude suggest that clastic  
293 injectites can be viewed as scale invariant. This is a powerful implication as exhumed  
294 analogues need not be seismic-scale when other parameters such as geometry, tectonic  
295 setting and connection to the contemporaneous seabed differ from the subsurface systems.  
296 Rather a range of outcrop observations can be used to provide improved constraints on the  
297 sub-seismic injectite networks, and connectivity, to better predict and model fluid flow during  
298 hydrocarbon production, or carbon capture and sequestration.

## 299 **References**

300 Ahmadi, Z.M., Sawyers, M., Kenyon-Roberts, S., Stanworth, C.W., Kugler, K.A., Kristensen, J.,  
301 Fugelli, E.M.G., 2003. 14 Palaeocene. In: Evans, D., Graham, C., Armour A., Bathurst, P. (Eds.),  
302 The Millennium Atlas: Petroleum Geology of the Central and Northern North Sea. Geological  
303 Society, London, 235-259.

304 Barnard, P.C., Bastow, M.A., 1991. Hydrocarbon generation, migration, alteration,  
305 entrapment and mixing in the Central and Northern North Sea. In: England, W.A, Fleet, A.J.  
306 (Eds.), Petroleum Migration, Geological Society London, Special Publication 59, 167-190.

307 Bentley, M., Smith, S., 2008. Scenario-based reservoir modelling: the need for more  
308 determinism and less anchoring. In: Robinson, A., Griffiths, P., Price, S., Hegre, J., Muggeridge,

- 309 A. (Eds.), *The Future of Geological Modelling in Hydrocarbon Development*, Geological Society  
310 London, Special Publication 309, 145-159.
- 311 Bussel, M.A., 1989. A simple method for the determination of the dilation direction of  
312 intrusive sheets. *Journal of Structural Geology* 11, 679-687.
- 313 Cartwright, J., 2010. Regionally extensive emplacement of sandstone intrusions: a brief  
314 review. *Basin Research* 22, 502-516.
- 315 Cartwright, J.A., Huuse, M., James, D., Hurst, A., Vetel, W., 2008. The geometry and  
316 emplacement of conical sandstone intrusions. *Journal of Structural Geology* 30, 854-867.
- 317 Cheret, T., Carrillat, A., 2004. Seismic Scale Sand Injectites in the North Sea. In: SPE Annual  
318 Technical Conference and Exhibition 26-29 September, Houston, Texas. Society of Petroleum  
319 Engineers. doi:10.2118/90375-MS
- 320 Chiarelli, A., Richey, J.F., 1984. Hydrodynamic flow in sedimentary basins. In: Durand, B. (Ed.),  
321 *Thermal phenomena in sedimentary basins*. Paris: Editions Technip, 175-187.
- 322 Cobain, S.L., Peakall, J., Hodgson, D.M., 2015. Indicators of propagation direction and relative  
323 depth in clastic injectites: Implications for laminar versus turbulent flow processes. *Geological*  
324 *Society of America Bulletin* 127, 1816-1830.
- 325 Cobain, S.L., Hodgson, D.M., Peakall, J., Shiers, M.N., 2017. An integrated model of clastic  
326 injectites and basin floor lobe complexes: Implications for stratigraphic trap plays. *Basin*  
327 *Research*, 29, 816-835.
- 328 Cobain, S.L., Hodgson, D.M., Peakall, J., Wignall, P.B., Cobain, M.R.D., 2018. A new  
329 macrofaunal limit in the deep biosphere revealed by extreme burrow depths in ancient  
330 sediments. *Scientific Reports*, 8, 261.
- 331 Cruden, A., Bungler, A., 2010. Emplacement dynamics of laccoliths, sills and dykes from  
332 dimensional scaling and mechanical models. In: Morgan, S., Horsman, E., de Saint Blanquat,  
333 M., Tikoff, M. (Eds.), *LASI 4 Conference: Physical Geology of Subvolcanic Systems: Laccoliths,*  
334 *Sills and Dykes*. Central Michigan University, 15-16

- 335 de Boer, W., Hurst, A., Rawlinson, P.B., 2007. Successful exploration of a sand injectites  
336 complex: Hamsun Prospect, Norway Block 24/9. In: Hurst, A., Cartwright, J. (Eds.), *Sand*  
337 *Injectites: Implications for Hydrocarbon Exploration and Production*: American Association of  
338 *Petroleum Geologists Memoir 87*, 65-78.
- 339 Duranti, D., Hurst, A., Bell, C., Groves, B., Hanson, R., 2002. Injected and remobilized Eocene  
340 sandstones from the Alba Field, UKCS: core and wireline log characteristics. *Petroleum*  
341 *Geoscience* 8, 99-107.
- 342 Galloway, W.E., Garber, J.L., Liu, X., Sloan, B.J., 1993. Sequence stratigraphic and depositional  
343 framework of the Cenozoic fill, Central and Northern North Sea Basin. In: J. R. Parker (Ed.),  
344 *Petroleum Geology Conference series: Proceedings of the 4<sup>th</sup> Conference*. Geological Society,  
345 London, 33-44.
- 346 Goodall, I., Lofts, J., Mulcahy, M., Ashton, M., Johnson, S., 1999. A sedimentological  
347 application of ultrasonic borehole images in complex lithologies: the Lower Kimmeridge Clay  
348 Formation, Magnus Field, UKCS. In: Lovell, M.A., Williamson, G., Harvey, P.K., (Eds.), *Borehole*  
349 *Imaging: applications and case histories*. Geological Society, London, *Special Publications 159*,  
350 203-225.
- 351 Gressier, J.B., Mourgues, R., Bodet, L., Mathieu, J.Y., Galland, O., Cobbold, P.R., 2010. Control  
352 of pore fluid pressure on depth of emplacement of magmatic sills: an experimental approach.  
353 *Tectonophysics* 489, 1-13.
- 354 Hubbard, S.M., Romans, B.W., Graham, S.A. (2007) An outcrop example of large-scale  
355 conglomeratic intrusions sourced from deep-water channel deposits, Cerro Toro Formation,  
356 Magallanes basin, southern Chile. In: *Sand Injectites: Implications for Hydrocarbon Exploration*  
357 *and Production*. In: Hurst, A. and Cartwright, J. (Eds.), *American Association of Petroleum*  
358 *Geologists Memoir 87*, 199-207.
- 359 Hubbert, M.K., 1937. Theory of scale models as applied to the study of geologic structures.  
360 *Geological Society of America Bulletin* 48, 1459-1520.



- 361 Hubbert, M.K., 1951. Mechanical basis for certain familiar geologic structures. Geological  
362 Society of America Bulletin 62, 355-372.
- 363 Hubbert, M.K., Willis, D.G., 1957. Mechanics of hydraulic fracturing. Petroleum Transactions  
364 of the American Institute of Mining Engineers 210, 153-168.
- 365 Hudec, M.R., Jackson, M.P.A., 2010. The salt mine: a digital atlas of salt tectonics: Austin TX,  
366 The University of Texas at Austin, Bureau of Economic Geology, Udden Book Series 5; Tulsa  
367 OK, American Association of Petroleum Geologists, Memoir 99, 305 pp.
- 368 Hurst, A., Cartwright, J. A., Duranti, D., Huuse, M., Nelson, M., 2005. Sand injectites: an  
369 emerging global play in deep-water clastic environments. In: Doré, A. G., Vining, B. A. (Eds.),  
370 Petroleum Geology: North-West Europe and Global Perspectives—Proceedings of the 6th  
371 Petroleum Geology Conference. Geological Society, London 6, 133-144.
- 372 Hurst, A., Scott, A., Vigorito, M., 2011. Physical characteristics of sand injectites. Earth-Science  
373 Reviews 106, 215-246.
- 374 Huuse, M., Cartwright, J., Hurst, A., Steinsland, N., 2007. Seismic characterization of large-  
375 scale sandstone intrusions. In: Hurst, A., Cartwright, J. (Eds.), Sand Injectites: Implications for  
376 Hydrocarbon Exploration and Production: American Association of Petroleum Geologists  
377 Memoir 87, 21-35.
- 378 Huuse, M., Duranti, D., Steinsland, N., Guargena, C.G., Prat, P., Holm, K., Cartwright, J.A.,  
379 Hurst, A., 2004. Seismic characteristics of large-scale sandstone intrusions in the Paleogene of  
380 the South Viking Graben, UK and Norwegian North Sea. In: Davies, R.J., Cartwright, J., Stewart,  
381 S.A., Underhill, J.R., Lappin, M. (Eds.), 3D Seismic Technology: Application to the Exploration  
382 of Sedimentary Basins. Geological Society, London, Memoir 29, 263–277.
- 383 Jackson, C., Huuse, M., Barber, G., 2011. Geometry of wing-like clastic intrusions adjacent to  
384 a deep-water channel complex: Implications for hydrocarbon exploration and production.  
385 AAPG Bulletin 95, 559-584.

- 386 Jackson, M.P.A., Cramez, C., 1989. Seismic recognition of salt welds in salt tectonics regimes.  
387 In: Gulf of Mexico salt tectonics, associated processes, and exploration potential: SEPM Gulf  
388 Coast Section, 10th Annual research conference programme and abstracts, 66-71.
- 389 Jolly, R.J.H, Lonergan, L., 2002. Mechanisms and controls on the formation of sand intrusions.  
390 Journal of the Geological Society, London 159, 605-617.
- 391 Kavanagh, J.L., Menand, T., Sparks, R.S.J., 2006. An experimental investigation of sill formation  
392 and propagation in layered elastic media. Earth and Planetary Science Letters, 245, 799-813.
- 393 Kilhams, B., Hartley, A., Huuse, M., Davis, C., 2012. Characterizing the Paleocene turbidites of  
394 the North Sea: the Mey Sandstone Member, Lista Formation, UK central graben. Petroleum  
395 Geoscience 18, 337-354.
- 396 Kubala, M., Bastow, M., Thompson, S., Scotchman, I., Oygard, K., 2003. Geothermal regime,  
397 petroleum generation and migration. In: Evans, D., Graham, C., Armour A., Bathurst, P. (Eds.),  
398 The Millennium Atlas: Petroleum Geology of the Central and Northern North Sea. Geological  
399 Society, London, 289-315.
- 400 Lonergan, L., Quine, M., Borlandelli, C., Flanagan, K., Taylor, S., 2007. The three-dimensional  
401 geometry of sandstone injection complexes in the Gryphon Field, United Kingdom North Sea.  
402 In: Hurst, A., Cartwright, J. (Eds.), Sand Injectites: Implications for Hydrocarbon Exploration  
403 and Production: American Association of Petroleum Geologists Memoir 87, 103-112.
- 404 Løseth, H., Rodrigues, N., Cobbold, P.R., 2012. World's largest extrusive body of sand?  
405 *Geology*, 40, 467-470.
- 406 Magee, C., Maharaj, S.M., Wrona, T., Jackson, C.A-L., 2015. Controls on the expression of  
407 igneous intrusions in seismic reflection data. *Geosphere* 11, 1024-1041.
- 408 McCaffrey, K.J.W., Petford, N., 1997. Are granitic intrusions scale invariant? *Journal of the*  
409 *Geological Society* 154, 1-4.

- 410 Monnier, D., Imbert, P., Gay, A., Mourgues, R., Lopez, M., 2014. Pliocene sand injectites from  
411 a submarine lobe fringe during hydrocarbon migration and salt diapirism: a seismic example  
412 from the Lower Congo Basin. *Geofluids* 14, 1–19.
- 413 Mourgues, R., Cobbold, P.R., 2003. Some tectonic consequences of fluid overpressures and  
414 seepage forces as demonstrated by sandbox modeling. *Tectonophysics* 376, 75-97.
- 415 Mourgues, R., Bureau, D., Bodet, L., Gay, A., Gressier, J.B., 2012. Formation of conical fractures  
416 in sedimentary basins: Experiments involving fluids and implications for sandstone intrusion  
417 mechanisms. *Earth and Planetary Science Letters* 313-314, 67-78.
- 418 Mudge, D.C., 2014. Regional controls on Lower Tertiary sandstone distribution in the North  
419 Sea and NE Atlantic margin basins. In: McKie, T., Rose, P.T.S, Hartley, A.J., Jones, D.W.,  
420 Armstrong, T.L. (Eds.), *Tertiary Deep-Marine Reservoirs of the North Sea Region*. Geological  
421 Society, London, Special Publications 403, 403-5.
- 422 Mudge, D.C., Copestake, P., 1992. Lower Palaeogene stratigraphy of the northern North Sea.  
423 *Marine and Petroleum Geology* 9, 287-301.
- 424 Nicholson, R., Pollard, D.D., 1985. Dilation and linkage of en-echelon cracks. *Journal of*  
425 *Structural Geology* 7, 583-590.
- 426 Østmo, S., McFadzean, P., Silcock, S., Spjuth, C., Sundvor, E., Letki, L.P., Clark, D., 2014.  
427 Improved reservoir characterization by multisensor towed streamer seismic data at the  
428 Mariner Field. *76th EAGE Conference & Exhibition, Extended Abstracts*.
- 429 Palladino, G., Alsop, G.I., Grippa, A., Zvirtes, G., Phillip, R.P., Hurst, A., 2018. Sandstone-filled  
430 normal faults: A case study from Central California. *Journal of Structural Geology* 110, 86-101.
- 431 Parize, O., Beaudoin, B., Champenhet, J-M., Friès, G., Imbert, P., Labourdette, R., Paternoster,  
432 B., Rubino, J-L., Schneider, F., 2007a. A methodological approach to clastic injectites: from  
433 field analysis to seismic modelling – examples of the Vocontian Aptian and Albian injectites  
434 (Southeast France). In: Hurst, A., Cartwright, J. (Eds.), *Sand Injectites: Implications for*

- 435 Hydrocarbon Exploration and Production. American Association of Petroleum Geologists  
436 Memoir 87, 173-183.
- 437 Parize, O., Beaudoin, B., Eckert, S., Hadj-Hassen, F., Tijani, M., de Fouquet, C., Vandromme, R.,  
438 Fries, G., Schneider, F., Su, F., Trouiller, A., 2007b. The Vocontian Aptian and Albian  
439 syndepositional clastic sills and dikes: A field-based mechanical approach to predict and model  
440 the early fracturing of marly-limy sediments. In: Hurst, A., Cartwright, J. (Eds.), Sand Injectites:  
441 Implications for Hydrocarbon Exploration and Production. American Association of Petroleum  
442 Geologists Memoir 87, 163-172.
- 443 Polteau, S., Mazzini, A., Galland, O., Planke, S., Malthe-Sørenssen, A., 2008. Saucer-shaped  
444 intrusions: Occurrences, emplacement and implications. Earth and Planetary Science Letters  
445 266, 195-204.
- 446 Rodrigues, N., Cobbold, P.R., Løseth, H., 2009. Physical modelling of sand injectites.  
447 Tectonophysics 474, 610-632.
- 448 Ross, J.A., Peakall, J., Keevil, G.M., 2014. Facies and flow regimes of sandstone-hosted  
449 columnar intrusions: insights from the pipes of Kodachrome Basin State Park. Sedimentology  
450 61, 1764–1792.
- 451 Rowe, C.A., Mustard, P.S., Mahoney, J.B., Katnick, D.C., 2002. Oriented clastic dike swarms as  
452 indicators of paleoslope? An example from the upper Cretaceous Nanaimo Group, Canada.  
453 Journal of Sedimentary Research 72, 192-200.
- 454 Satur, N., Hurst, A., 2007. Sand-injection structures in deep-water sandstones from the Ty  
455 Formation (Paleocene), Sleipner Field, Norwegian North Sea. In: Hurst, A., Cartwright, J. (Eds.),  
456 Sand Injectites: Implications for Hydrocarbon Exploration and Production. American  
457 Association of Petroleum Geologists Memoir 87, 113-117.
- 458 Schofield, N.J., Brown, D.J., Magee, C., Stevenson, C.T., 2012a. Sill morphology and  
459 comparison of brittle and non-brittle emplacement mechanisms. Journal of the Geological  
460 Society 169, 127-141.

- 461 Schofield, N.J., Heaton, L., Holford, S.P., Archer, S.G., Jackson, C.A-L., Jolley, D.W., 2012b.  
462 Seismic imaging of 'broken bridges': linking seismic to outcrop-scale investigations of intrusive  
463 magma lobes. *Journal of the Geological Society* 169, 421-426.
- 464 Scholz, C.H., Aviles, C.A., 1986. The fractal geometry of faults and faulting. In: Das, S.,  
465 Boatwright, J., Scholz, C.H. (Eds.), *Earthquake Source Mechanics*. American Geophysical  
466 Union, Geophysical Monograph 37, 147-156.
- 467 Schultz, R.A., Soliva, R., Okubo, C.H., Mège, D., 2010. Fault populations. In: Watters, T.R.,  
468 Schultz, R.A. (Eds.), *Planetary Tectonics*, Cambridge University Press, 457-510.
- 469 Schwab, A.M., Jameson, E.W., Townsley, A., 2015. Volund Field: development of an Eocene  
470 sandstone injection complex, offshore Norway. In: McKie, T., Rose, P.T.S., Hartley, A.J., Jones,  
471 D.W., Armstrong, T.L. (Eds.), *Tertiary Deep-Marine Reservoirs of the North Sea Region*.  
472 Geological Society, London, Special Publications 403, 247-260.
- 473 Scott, A., Vigorito, M., Hurst, A., 2009. The process of sand injection: internal structures and  
474 relationships with host strata (Yellowbank Creek Injectite Complex, California, U.S.A.). *Journal*  
475 *of Sedimentary Research* 79, 568-583.
- 476 Scott, A., Hurst, A., Vigorito, M., 2013. Outcrop-based reservoir characterization of a  
477 kilometer-scale sand-injectite complex. *AAPG Bulletin* 97, 309-343.
- 478 Sigmundsson, F., Hooper, A. *et al.*, 2015. Segmented lateral dyke growth in a rifting event at  
479 Bárðarbunga volcanic system, Iceland. *Nature* 517, 191-195. Surlyk, F., Noe-Nygaard, N., 2001.  
480 Sand remobilisation and intrusion in the Upper Jurassic Hareelv Formation of East Greenland.  
481 *Bulletin of the Geological Society of Denmark* 48, 169-188.
- 482 Thomson, K., 2007. Determining magma flow in sills, dykes, and laccoliths and their  
483 implications for sill emplacement mechanisms. *Bulletin of Volcanology* 70, 183-201.
- 484 Thomson, K., Schofield, N., 2008. Lithological and structural controls on the emplacement and  
485 morphology of sills in sedimentary basins. In: Thomson, K., Petford, N., (Eds.), *Structure and*

- 486 emplacement of high-level magmatic systems. Geological Society, London, Special  
487 Publications 302, 31-44.
- 488 Totake, Y., Butler., R.W.H., Bond, C.E., Tokunaga, H., Aziz, A., 2018. Entrained sand generates  
489 fault-plane reflections on a deep-water thrust zone. *Geology* 46, 1039-1042.
- 490 Townsley, A., Jameson, E.W., Schwab, A., 2012. The Volund Field – Developing a unique sand  
491 injection complex in offshore Norway. *74th EAGE Conference & Exhibition*, Extended  
492 Abstracts.
- 493 Vigorito, M., Hurst, A., 2010. Regional sand injectite architecture as a record of pore-pressure  
494 evolution and sand redistribution in the shallow crust: insights from the Panoche Giant  
495 Injection Complex, California. *Journal of the Geological Society* 167, 889-904.
- 496 Vigorito, M., Hurst, A., Cartwright, J.A., Scott, A., 2008. Architecture of a sand injectite  
497 complex: implications for origin and timing. *Journal of the Geological Society* 165, 609-612.
- 498 Wibberley, C.A.J., Petit, J-P, Rives, T., 1999. Mechanics of high displacement gradient faulting  
499 prior to lithification. *Journal of Structural Geology* 21, 251-257.

500

501 **Table and figure captions**

502 **Table 1.** *Quantitative analysis of 14 bowl structures*

503 2D reflection seismic profiles were taken at intervals of 50 m along both ILs and XLs for 14  
504 bowl structures and the underlying Maureen Formation: plan view area (m<sup>2</sup>), perimeter (m),  
505 XL transect length (m), IL transect length (m), depth of top Maureen Formation (IL) (m), top  
506 Maureen Formation to base bowl vertical distance (IL) (m), depth to base bowl (IL) (m), depth  
507 to top bowl (IL) (m), vertical depth of bowl (m), depth of top Maureen Formation (XL) (m), top  
508 Maureen Formation to base bowl vertical distance (XL) (m), depth to base bowl (XL) (m), depth  
509 to top bowl (XL) (m), vertical depth of bowl (m).

510 **Fig. 1.** (A) North Sea Basin showing present day distribution of Palaeocene-Lower Eocene  
511 sandstone in yellow (adapted from Mudge, 2014) and locations of large scale sandstone  
512 injectites in the Palaeogene of the Northern North Sea outlined in red (after Huuse *et al.*,  
513 2007). (B) Stratigraphy of the North Sea case study (adapted from Ahmadi *et al.*, 2003).

514 **Fig. 2.** Example seismic sections through the study area. (A) Plan view of the study area  
515 showing extent of the Maureen Formation in pale grey. Black areas and the dashed line  
516 denote where Maureen is absent, and darker grey represents mapped sands within the Lista  
517 Formation. (B) Depth map in plan view of sands within the Lower Lista Formation and  
518 polygons outlining each mapped bowl feature. Yellow lines represent sections shown in Figure  
519 2C-F. (C-F) Seismic cross-sections through mapped sands; yellow line is the top Maureen  
520 Formation pick, pink line picks base sand in Lower Lista Formation shale. (C) Section A-A';  
521 steeply dipping, v-shaped bowl with complex internal sand architectures. (D) Section B-B'; v-  
522 shaped bowl where base of bowl is in contact with the top of the Maureen Formation. (E)  
523 Section C-C'; 5 km long section cutting through several outlined polygons (Fig. 2B). (F) Section  
524 through several bowl structures and well log A used to correlate sand bodies.

525 **Fig. 3.** Gamma Ray (GR) well log calibration to seismic interpretation, orange colour denotes  
526 low GR, primarily associated with higher sand content. (A) Profile through Bowl 5 (Fig. 2B),

527 where the underlying Maureen Formation shows thick sand packages, overlying thin sand units  
528 interpreted as injectites. **(B)** Western edge of Bowl 5, where the Maureen Formation is picked  
529 out by high sand content, and the edge of the bowl shows multiple, thin sands interpreted as  
530 injectites. **(C)** Edge of Bowl 5, sand bodies appear to have pinched out. Some sand layers of  
531 unknown origin higher up in stratigraphy.

532 **Fig. 4.** Geometric properties and vertical position of the mapped sands. **(A)** Vertical depth to  
533 base of each bowl and depth from base of bowl to the top of the Maureen Formation. **(B)**  
534 Bowl height *versus* width, showing low to moderate degree of variability in height through  
535 bowls of different widths. **IL = inline, XL = cross line.**

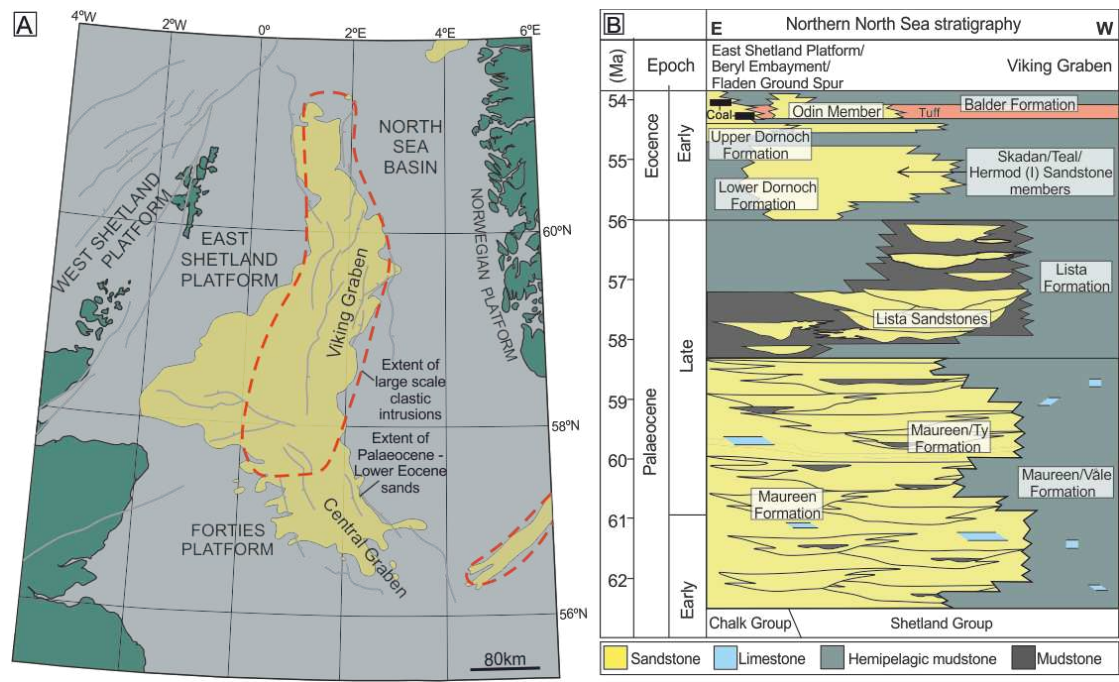
536 **Fig. 5.** **(A)** Representative reflection seismic section taken through the case study area. **(B)**  
537 Simplified interpretation of depleted parent sand (Maureen Fm.) and resultant injected sand.

538 **Fig. 6.** Time steps of parent sand depleting as injectites form. **(A)** T1: pre-injection, fan sands  
539 remain unconsolidated and become overpressured as overlying shale deposited. **(B)** T2:  
540 parent sand starts to drain and deform as it injects into overlying strata. Overlying shale starts  
541 to deform in response to sand draining and injecting. **(C)** T3: injectites cease propagating with  
542 development of a sand 'weld', resulting in a large area of parent sand depleted and forming a  
543 "channel-like" cross-sectional shape.

544 **Fig. 7.** Photographs of clastic injectites of same grain-size (fine and medium grain sand) and  
545 geometry (dykes and sills) across a wide range of scales. **(A)** Photograph from a Palaeocene  
546 succession, North Sea. **(B)** and **(C)** Photographs from the Fort Brown Formation, South Africa.  
547 **(D)** Photograph from Miocene exposures in the Austral Basin, Tierra del Fuego, Patagonia,  
548 Argentina.

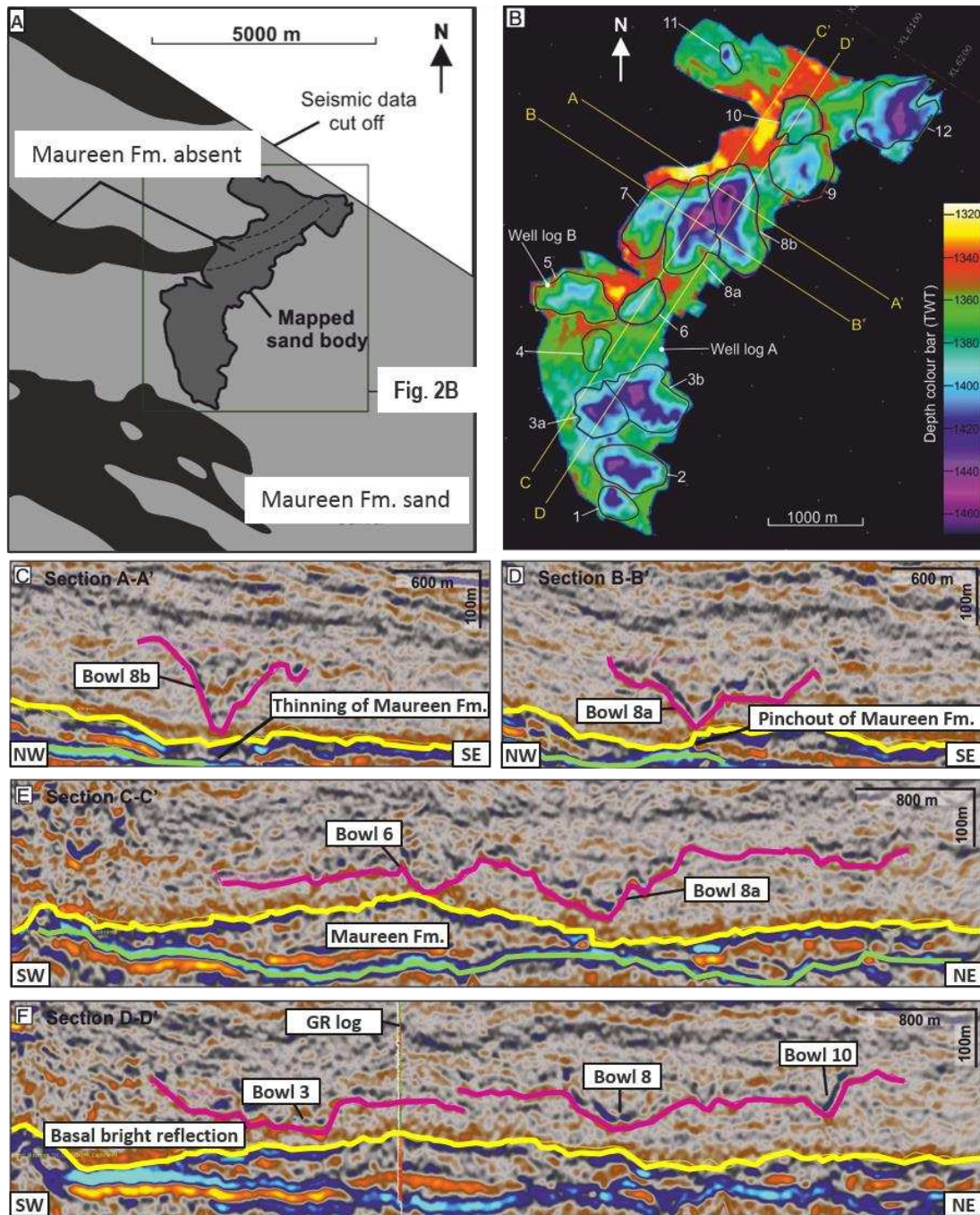
549 **Fig. 8.** **(A)** 3D reservoir modelling process for a single geological model (adapted from Bentley  
550 and Smith 2008). **(B)** Same model with sub-seismic injectites providing vertical connectivity  
551 between reservoir units.





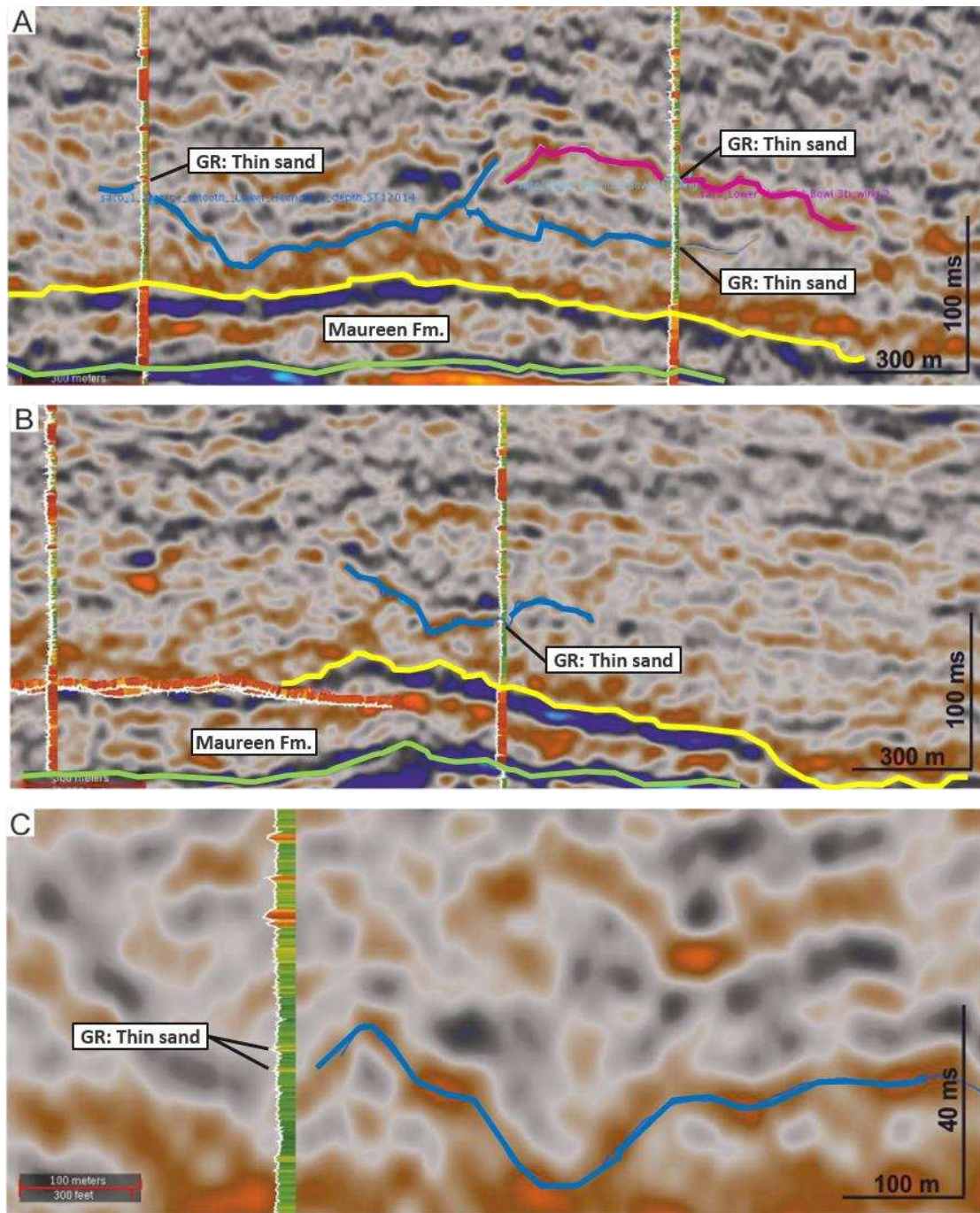
552

553 Figure 1



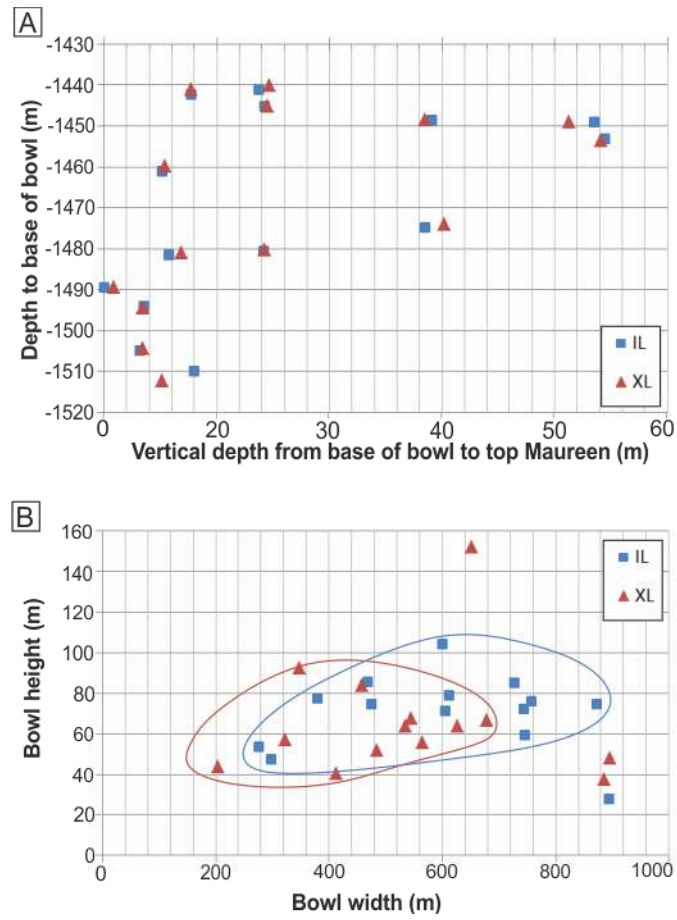
554

555 Figure 2



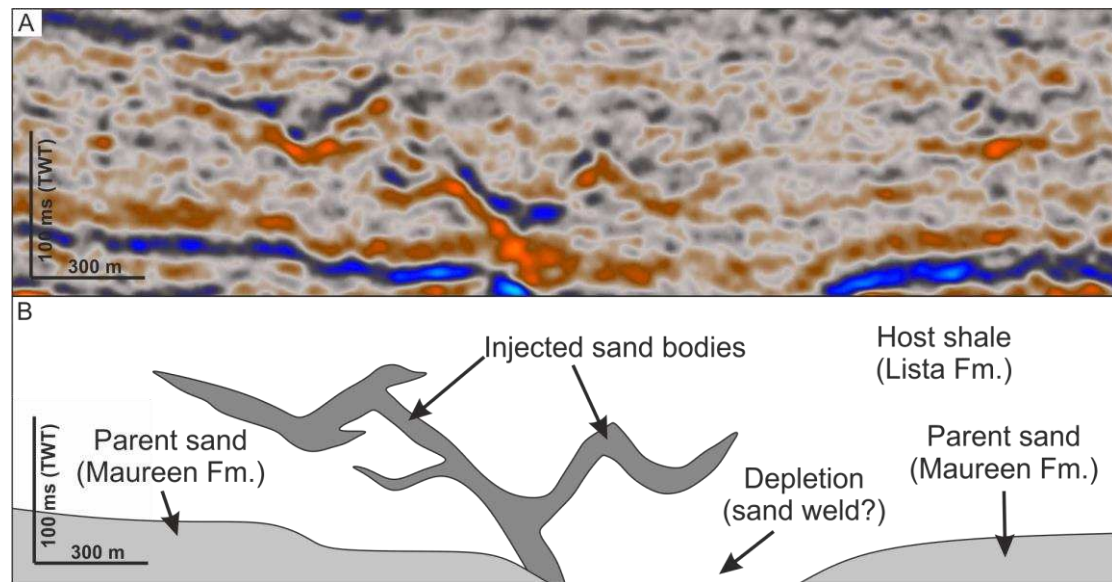
556

557 Figure 3



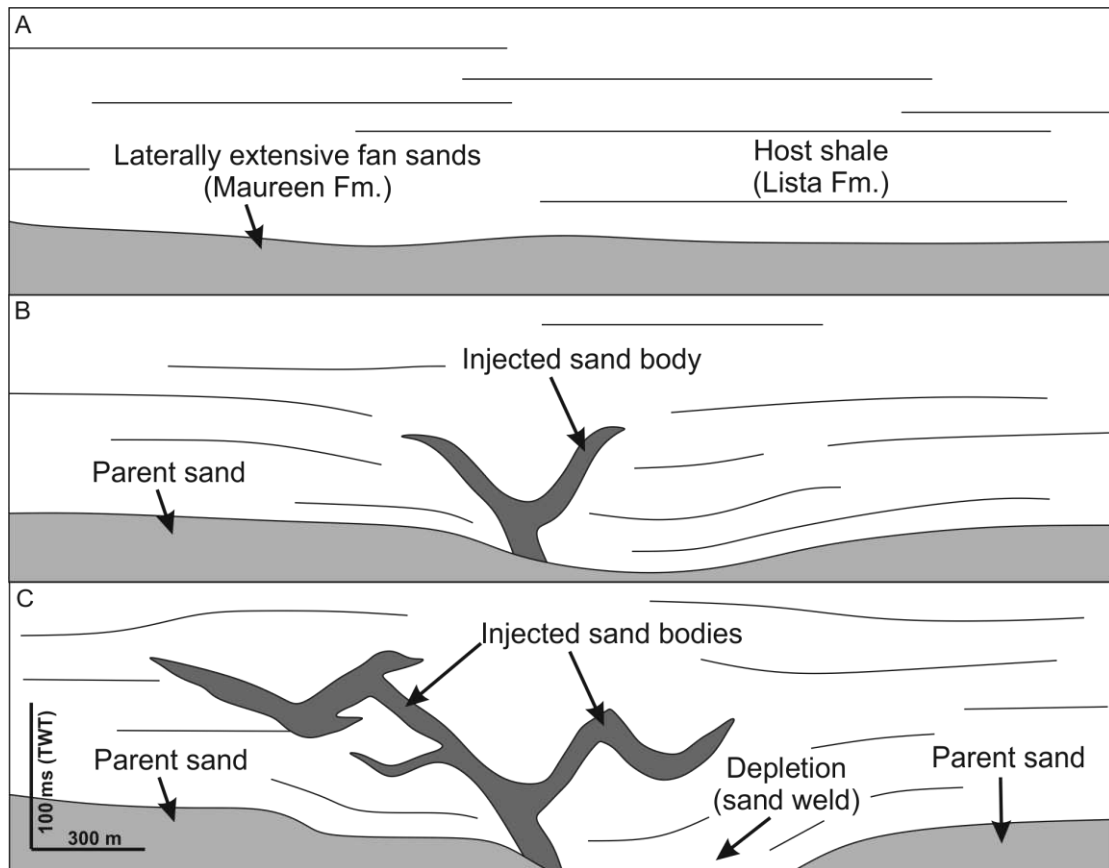
558

559 Figure 4



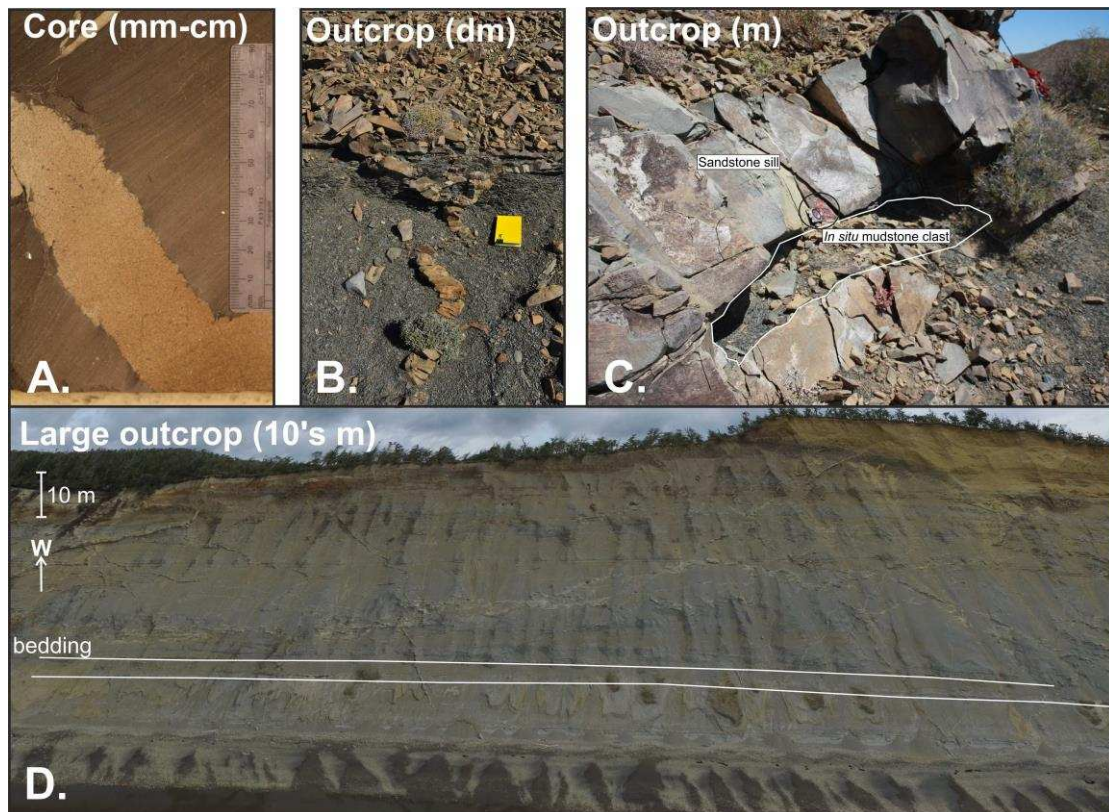
560

561 Figure 5



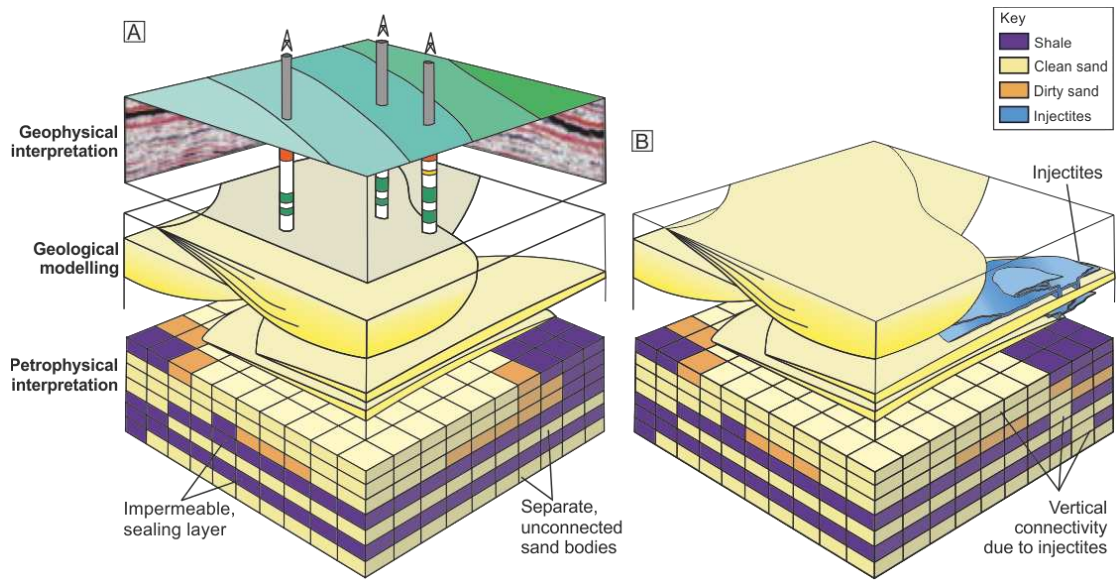
562

563 Figure 6



564

565 Figure 7



566

567 Figure 8